Journal of Neuroimmunology 330 (2019) 143–151

Contents lists available at ScienceDirect

Journal of Neuroimmunology

journal homepage: www.elsevier.com/locate/jneuroim

2′-Hydroxy-5′-methoxyacetophenone attenuates the inflammatory response in LPS-induced BV-2 and RAW264.7 cells via NF-κB signaling pathway

YuanYuan Zhang[a,b], ChengYong Li[a,c], ChunXia Zhou[b,c], PengZhi Hong[b], Yi Zhang[b], ShengLi Sun[a], Zhong-Ji Qian[a,c,*]

[a] School of Chemistry and Environment of Chemistry and Environment, Guangdong Ocean University, Zhanjiang 524088, China
[b] College of Food Science and Technology, Guangdong Ocean University, Zhanjiang 524088, China
[c] Shenzhen Institute of Guangdong Ocean University, Shenzhen 518108, China

ARTICLE INFO

Keywords:
Hippocampus kuda
Anti-inflammation
2′-Hydroxy-5′-Methoxyacetophenone
NF-Kb
Molecular docking

ABSTRACT

Seahorse has been used as a traditional medicine in Southeast Asian countries for a long time. A compound, 2'-Hydroxy-5′-Methoxyacetophenone (2H5M) isolated from seahorse, *Hippocampus kuda*, was tested for its anti-inflammatory effect in lipopolysaccharides (LPS)-stimulated BV-2 cells and RAW264.7 cells. MTT assay indicated that 2H5M has no cytotoxicity on two kinds of cells. The concentration of nitric oxide (NO) measured by Griess Reaction System showed that 2H5M could significantly inhibit the NO concentration. The ELISA results showed that 2H5M could suppress the secretion of TNF-α in a dose-dependent manner. Moreover, western blot analysis was utilized to measure the protein levels of inducible nitric oxide synthase (iNOS) and cyclooxygenase-2 (COX-2), mitogen-activated protein kinase (MAPK) and nuclear factor-kappa B (NF-κB) signaling pathways. Electrophoretic mobility shift assay (EMSA) demonstrated that 2H5M reduced NF-κB DNA binding activity. Furthermore, the molecular docking study showed that 2H5M can form active sites with NF-κB. Collectively, these results indicated that 2H5M possesses anti-inflammatory effects and may have a potential application in inflammatory disorders in the future.

1. Introduction

Inflammation refers to a complex biological response to micro-circulation induced by harmful stimuli, infections or injuries. It is initiated by a series of soluble mediators including complements, chemokines, cytokines and ROS released from inflammation-related cells, which can destroy the cause of inflammation (Lo Faro et al., 2014). However, over-expressed or prolonged inflammation can be a potent trigger for many diseases rather than a beneficial event, which is to blame for many diseases, including cancer, rheumatoid arthritis, chronic asthma, multiple sclerosis, obesity, autoimmune disease, diabetes, inflammatory bowel disease and cardiovascular diseases (Tsaryk et al., 2013). When it comes to brain, neuro-inflammation are considered as pathogenesis of neurodegenerative diseases (Chen et al., 2016).

Microglia cells are differentiated from extra-embryonic yolk sac progenitors and macrophages are derived from monocyte. However, they have many similar molecules on cell surfaces (Ginhoux et al., 2013). Microglia cells occupies 5–12% of total glial cells in murine and 0.5%–16.6% in human (Mammana et al., 2018). Under normal conditions, macrophages are blocked by blood-brain barrier (BBB) to enter the brain parenchyma, whereas, they will transfer to the brain and differentiate to pro-inflammatory phenotype when the BBB are infected or damaged, which may have a relationship with acute or chronic inflammation (Minogue, 2017). And macrophages/microglia oriented treatments have been emerged in the field of neurodegenerative disorders (Sevenich, 2018). In addition, for screening anti-inflammatory lead compounds, the BV-2 and/or RAW264.7 are stimulated by LPS to determine whether they can suppress the protein expressions of iNOS and COX-2 (Cheung et al., 2016). LPS could activate inflammatory responses and immune dysfunctions (Li et al., 2017).

NF-κB, a protein complex, has long been considered as a classical pathway to modulate inflammatory response. In general, NF-κB is located in the cytoplasm and sequestered by a family of inhibitory proteins known as inhibitors of κB (IκBs) (Ye et al., 2018). However, the release of pro-inflammatory factors or LPS triggers a cascade of signaling events in NF-κB pathway. Subsequently, the unbounded p65 dissociates from IκBα and then translocated to the nucleus, where it activates transcription of its target genes (Li et al., 2018).

Seahorse has been used as a traditional medicine in Southeast Asian countries for a long time. Traditionally, it has the potential to treat

* Corresponding author at: School of Chemistry and Environment of Chemistry and Environment, Guangdong Ocean University, Zhanjiang 524088, China.
E-mail address: zjqian78@163.com (Z.-J. Qian).

https://doi.org/10.1016/j.jneuroim.2019.03.009
Received 15 February 2019; Received in revised form 11 March 2019; Accepted 11 March 2019

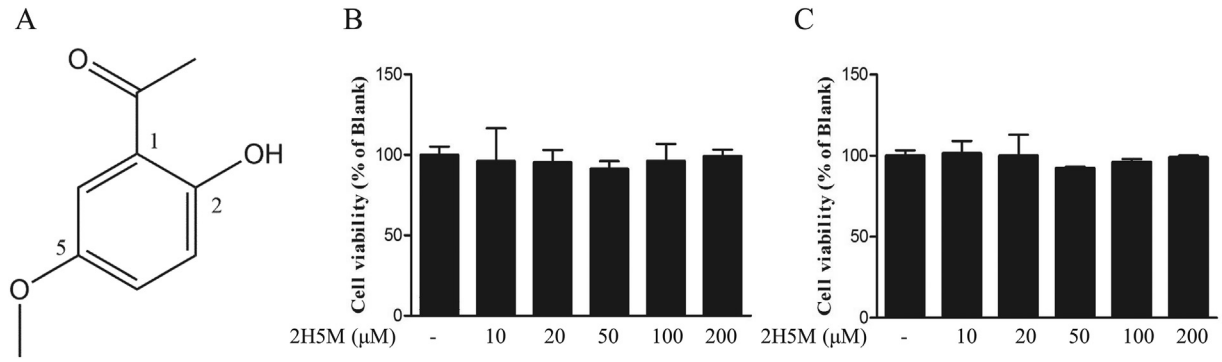

Fig. 1. Structure of 2'-Hydroxy-5′-methoxyacetophenone (A) and the cytotoxicity of 2H5M on BV-2 cells (B) and RAW 264.7 cells (C). Cells were exposed to varying concentrations of 2H5M and the cell viability was assesses by MTT assay. The results represent the mean ± S.D. (n = 3). There no significance among all tested groups.

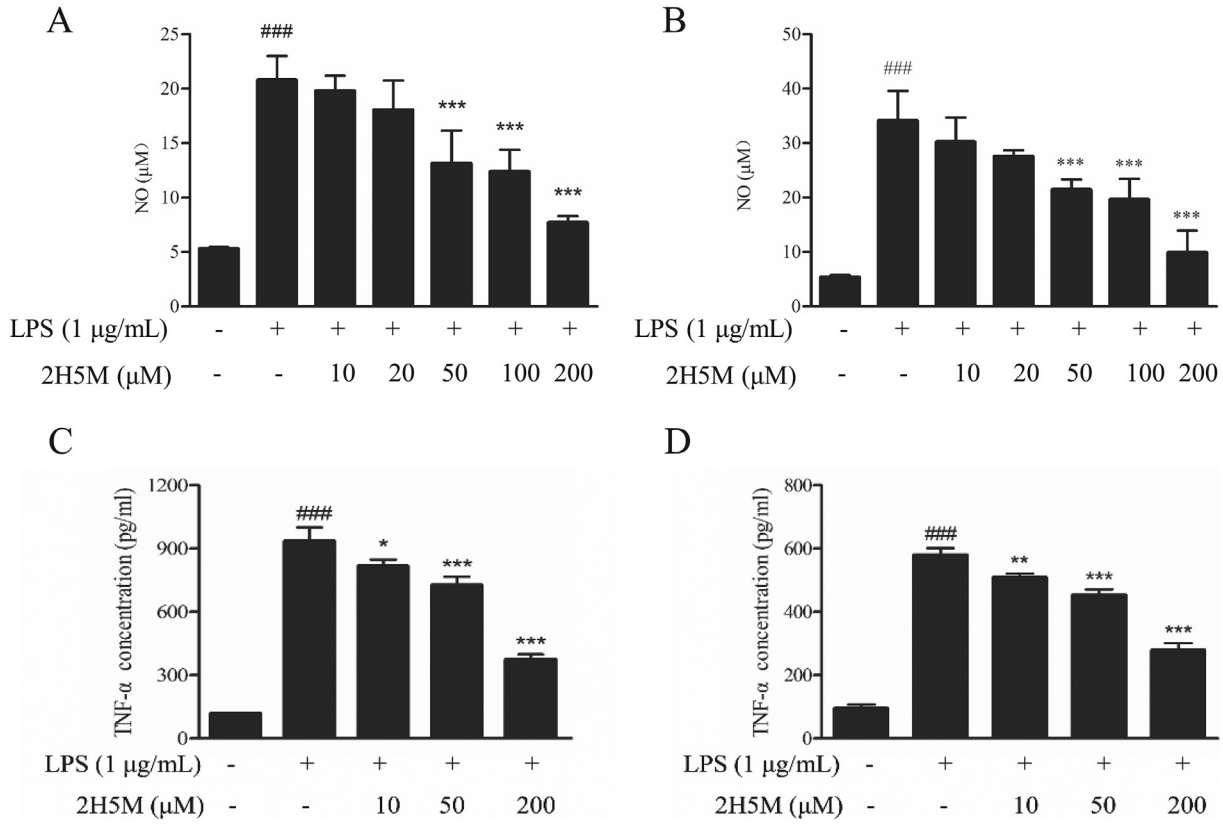

Fig. 2. Effect of 2H5M on the production of NO and TNF-α in LPS-induced BV-2 cells (A and C) and RAW 264.7 cells (B and D). Cells exposed to varying concentrations of 2H5M and then induced by LPS (1 μg/mL). Using Griess Reagents System to detect the concentration of NO induced in all groups. And the level of TNF-α was determined by ELISA. The results represent the mean ± SD (n = 3). ### p < .001, # p < .05, compared untreated cells; *** p < .001, ** p < .01 compared with LPS-treated cells.

infertility, baldness, asthma and arthritis (Zhang et al., 2017). Recently, several studies reported that seahorse possesses various biological activities, including anti-oxidative (Qian et al., 2008, 2012; Oh et al., 2018), anti-fatigue (Guo et al., 2017; Kang et al., 2017), promoting cell differentiation (Ryu et al., 2010; Muthuramalingam et al., 2019), neuro-inflammatory protective (Himaya et al., 2011) and anti-inflammatory effects (Chen et al., 2015; Neranjan Tharuka et al., 2019). Among, it has been found that 1-(5-bromo-2-hydroxy-4-methoxyphenyl) ethanone and paeonol are anti-inflammatory active component in the sea horse *H. kuda* Bleeler. Also, the 2'-Hydroxy-5′-Methoxyacetophenone (2H5M) was isolated. Previously, it has been found that 2H5M has acaricidal activity (Kim et al., 2013), however, to date, there are still no further research to report about other activities of 2H5M. Therefore, in this study, the investigated the anti-inflammatory effects of 2H5M on LPS-induced BV-2 and RAW264.7 cells.

2. Materials and methods

2.1. Materials

^{13}C NMR (400 MHz) and ^{1}H NMR (100 MHz) and spectra were recorded on a JEOL JNM-ECP 400 NMR spectrometer (JEOL, Japan), using $CDCl_3$ (1D, 12.75 ppm in ^{1}H and 113–9 ppm in ^{13}C NMR). Silica gel 60 (230–400 mesh, Merck, Germany), and thin-layer chromatography (TLC) plates (Kieselgel 60F254, 0.25 mm, Merck) were used for column chromatography and analytical TLC, respectively.

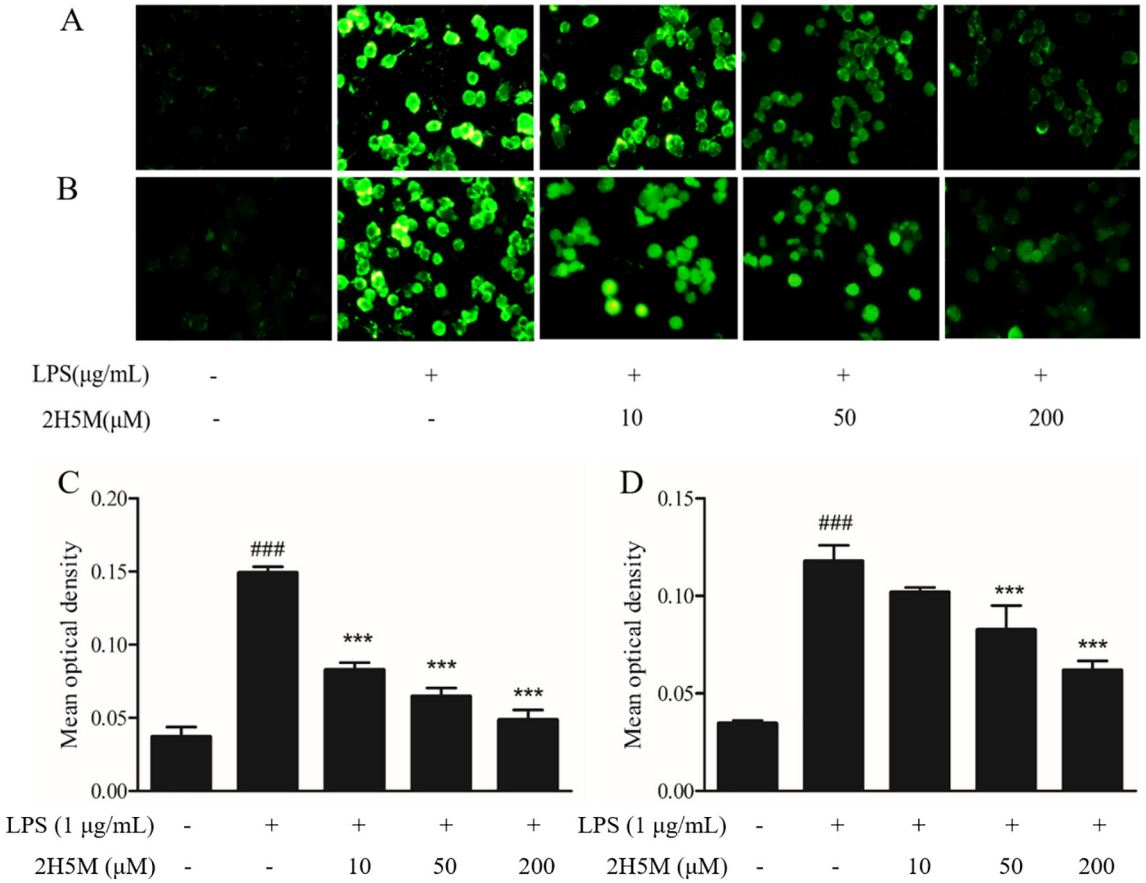

Fig. 3. Effect of 2H5M on ROS production in LPS-induced BV-2 cells (A) and RAW 264.7 cells (B) and the Mean optical density were shown in C and D, respectively. The cells were pre-treated with or without 2H5M and then were stimulated with LPS (1 μg/mL) for another 24 h. The DCF fluorescent probe were labeled to the cell for 30 min and the ROS production was visualized using inverted fluorescence microscope. ### $p < .001$, compared untreated cells; *** $p < .001$, compared with LPS-treated cells.

Commercial specific complete Dulbecco's modified eagle's medium (DMEM), penicillin and streptomycin were purchased from GIBCO (Carlsbad, USA), LPS and 3-(4, 5-dmethylthiazol-2-yl)-2, 5-diphenyl-2H-tetrazolium bromide (MTT) were purchased from Sigma-Aldrich (St. Louis, USA), Primary antibodies and secondary antibodies were purchased from Santa Cruz Biotechnology (Santa Cruz, USA), Dylight 488 secondary antibody was acquired from Abbkine (CA, USA), 2, 7-Dichlorodi-hydrofluorescein diacetate (DCFH-DA) was obtained from Solarbio Life Science (Beijing, China), TNF-α Elisa kit, Nuclear and Cytoplasmic Extraction Kit, Chemiluminescent EMSA Kit were obtained from Beyotime Biotechnology (Shanghai, China). Other chemicals were of analytic grade.

2.2. Extraction and isolation

Dry seahorses (*Hippocampus kuda*) were purchased from Zhoushan Island (Zhejiang, China) in October 2005. 2H5M was prepared according to a previously described method (Himaya et al., 2011). The *Hippocampus kuda* was ground into powder and refluxed with MeOH, and the solvent was evaporated in vacuo to obtain the crude MeOH extract. The extract was subjected to silica gel flash chromatography by eluting with n-hexane/EtOAc/MeOH (gradient), and got 10 main fractions. One of the fraction was purified over Silica gel repeatedly to obtain the purified compound.

2.3. Cell culture and cell viability assay

RAW264.7 and BV-2 cells, obtained from the Cell Bank of Chinese Academy of Sciences (Shanghai, China), were cultured in DMEM containing 10% FBS and 1% penicillin/streptomycin at 37 °C in a humidified 5%-CO_2 incubator. The cytotoxicity of 2H5M on cells was assessed by MTT assay. Briefly, BV-2 and RAW264.7 cells were seeded at a density of 1×10^4 cells/well in 96-well plates and were treated with 2H5M (10, 20, 50, 100, and 200 μM) for 24 h. Then 100 μL MTT (1 mg/mL) was added into the wells. After 4 h, adding 100 μL DMSO to dissolve the formazan crystals and the absorbance at 540 nm were measured.

2.4. NO determination

BV-2 and RAW264.7 cells were seeded at a density of 5×10^4 cells/well in 96-well plates. The cells were pre-treated with 2H5M (10, 20, 50, 100, and 200 μM) for 1 h, and then activated by LPS (1 μg/mL) for another 24 h. The production of NO was measured using Griess Reagent System according protocol (Promega, Madison, USA).

2.5. TNF-α determination

The level of TNF-α was determined by ELISA. Briefly, BV-2 and RAW264.7 cells were seeded at 5×10^5 cells/well in 24-well plates for 24 h. The cells were pre-treated with 2H5M (10, 50, and 200 μM) for 1 h and then activated by LPS (1 μg/mL) for 24 h. The culture medium was collected and centrifuged at 3000 rpm for 20 min. The level of TNF-α in the culture medium was quantified using ELISA kit (Beyotime Biotechnology, China).

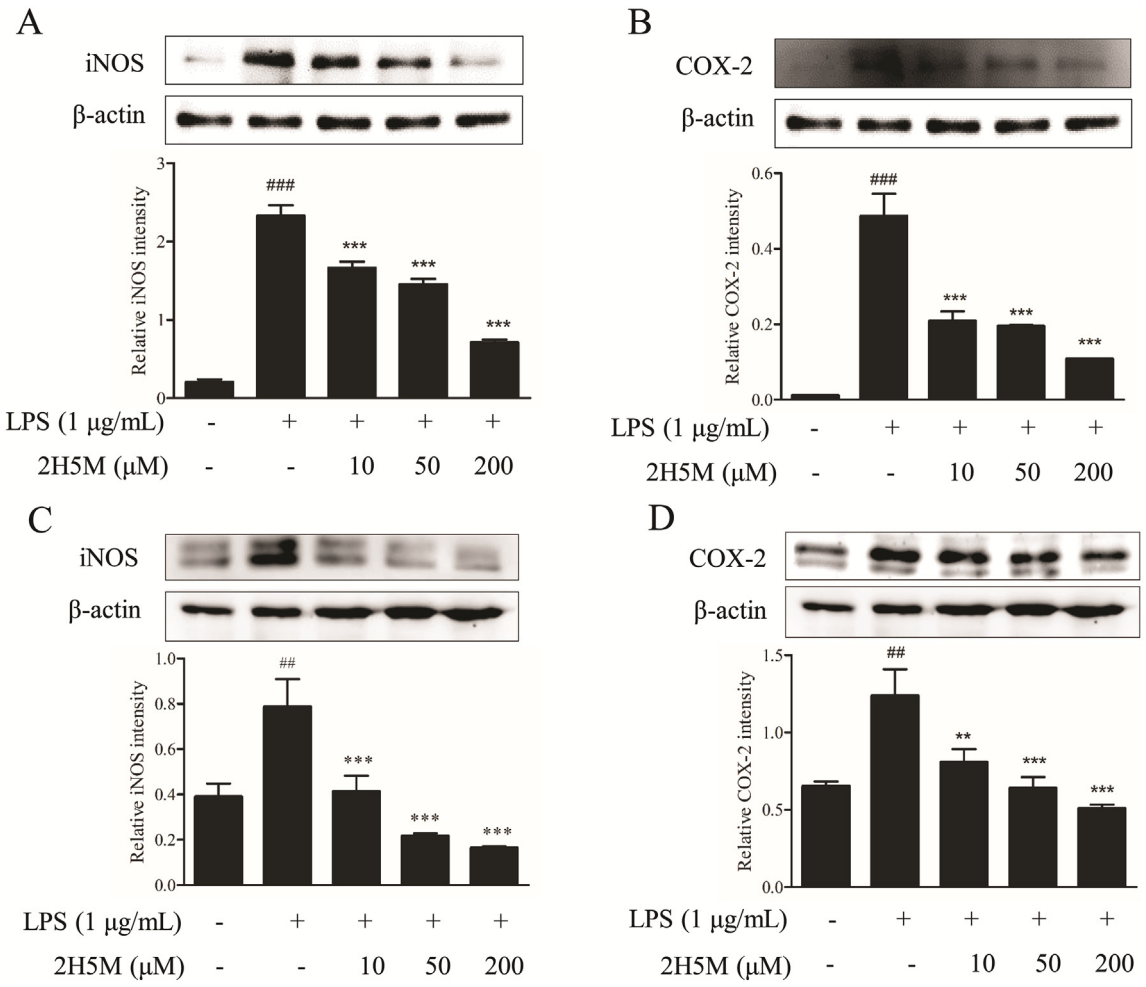

Fig. 4. Inhibitory effects of 2H5M on pro-inflammatory enzymes iNOS and COX-2 in BV-2 cells (A and B) and RAW 264.7 cells (C and D). Cells were exposed to varying concentrations of 2H5M with LPS. Protein expression was studied by western blotting and β-actin was function as control. ### $p < .001$, ## $p < .01$, compared untreated cells; *** $p < .001$, ** $p < .01$, compared with LPS-treated cells.

2.6. ROS determination

The accumulation of ROS was assessed by DCFH-DA. Briefly, the cells were seeded at density of 1×10^4 cells/well in 24-well plate and treated with 2H5M (10, 50, and 200 μM) for 1 h, then stimulated with LPS (1 μg/mL) for 24 h. The cells were rinsed with phosphate buffered saline (PBS) three times, and then were incubated with DCFH-DA (10 μM) for 30 min in the dark. After incubation, the cells were visualized by an inverted fluorescence microscope (Olympus Opticals, Tokyo, Japan).

2.7. Western blot analysis

BV-2 and RAW246.7 cells were seeded at a density of 5×10^6 cells/well in 6-well plates. The cells were pre-treated with 2H5M (10, 50, and 200 μM) for 1 h and then stimulated by LPS (1 μg/mL) for 24 h. The collected cells were rinsed thrice with cold PBS and lysed in RIPA buffer. Protein concentrations were determined using Pierce BCA Protein Assay Kit. Equal amounts of protein (20–40 μg) were separated electrophoretically using a 10% sodium dodecyl sulfate-polyacrylamide gel electrophoresis (SDS-PAGE), and then transferred onto nitrocellulose (NC) filter membranes (Amersham, USA). Membranes were then blocked with 5% skim milk and incubated with primary antibody and horseradish peroxidase (HRP)-conjugated secondary antibody. Blots were quantified by Amersham ECL Western Blotting Detection Kit.

2.8. EMSA assay

BV-2 and RAW264.7 cells were seeded at a density of 1×10^6 cells/well in 6-well plates and treated with 2H5M (10, 50, and 200 μM) for 1 h, then stimulated with LPS (1 μg/mL) for another 18 h. Nuclear extracts from cells were prepared with a Nuclear and Cytoplasmic Extraction Kit according to protocol. Nuclear protein (5 μg) was incubated with 0.2 μg of probe (5′-AGT TGA GGG GAC TTT CCC AGG C-3′). The reaction mixtures were electrophoresed through 6.5% polyacrylamide gel, and then transferred to a positive charge nylon membrane. After the transfer, the membrane was cross-linked and biotin-labeled DNA was detected using a Chemiluminescent EMSA Kit (Beyotime Biotechnology, China) according to instruction.

2.9. Immunocytochemistry

BV-2 and RAW246.7 cells were seeded at 5×10^4 cells/well in 24-well plates for 24 h. The cells were pre-treated with 2H5M (200 μM) for 1 h and then induced by LPS (1 μg/mL). After 24 h, cells were washed thrice with PBS and were fixed with 4% paraformaldehyde (PFA). Then, cells were permeabilized with 0.2% Triton X-100 (Sigma, USA). The cells were blocked with 5% bovine serum albumin (BSA) and then were incubated with anti-p65 antibody. After removed the primary antibody, the cell were washed again and incubated with Dylight 488 conjugated Goat Anti-Rabbit IgG secondary antibody (Abbkine, USA) in the dark. Finally, cells were stained with 100 ng/mL DAPI for 5 min before

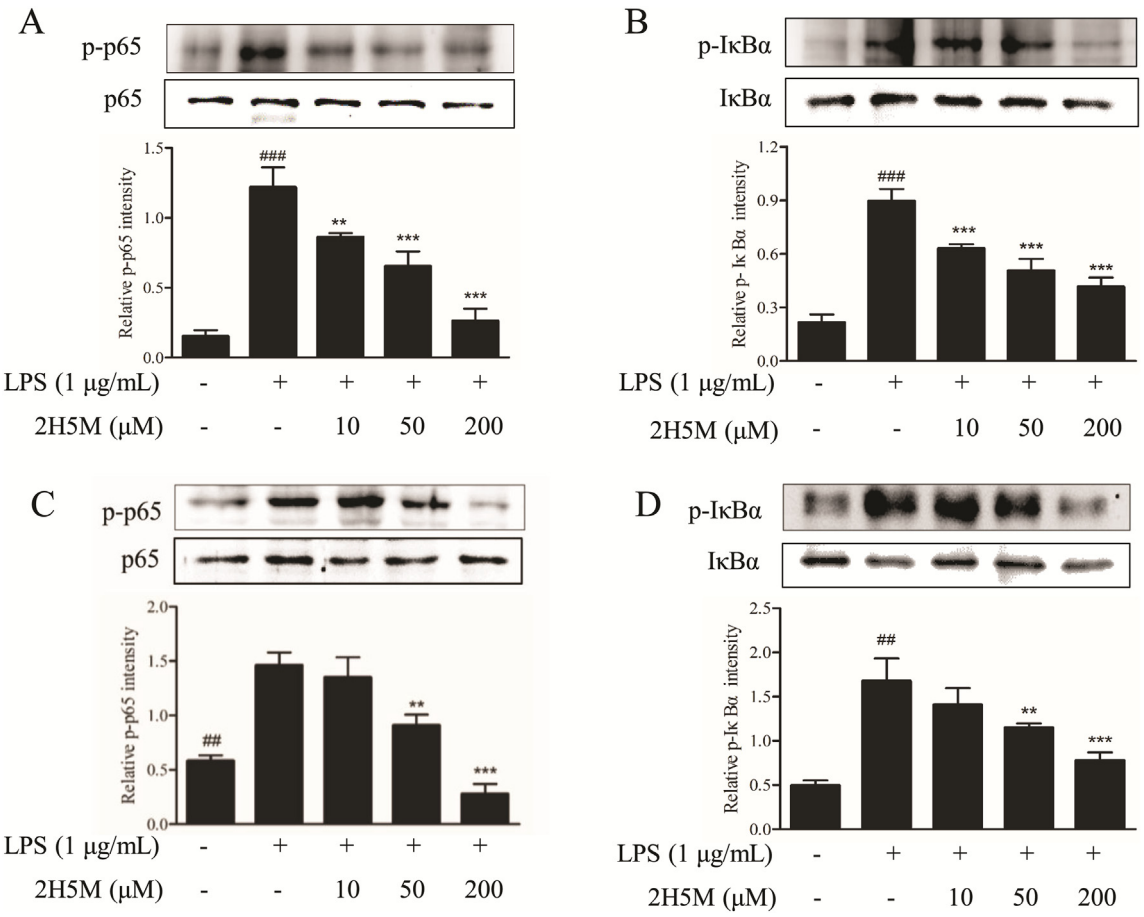

Fig. 5. Effects of 2H5M on the expression of NF-κB p65 and IκBα in LPS-induced BV-2 (A and B) and RAW 264.7 cells (C and D). Cells were exposed to varying concentrations of 2H5M with LPS. Protein expression was studied by western blotting and β-actin was function as control. ### $p < .001$, ## $p < .01$, compared untreated cells; *** $p < .001$, ** $p < .01$, * $p < .05$ compared with LPS-treated cells.

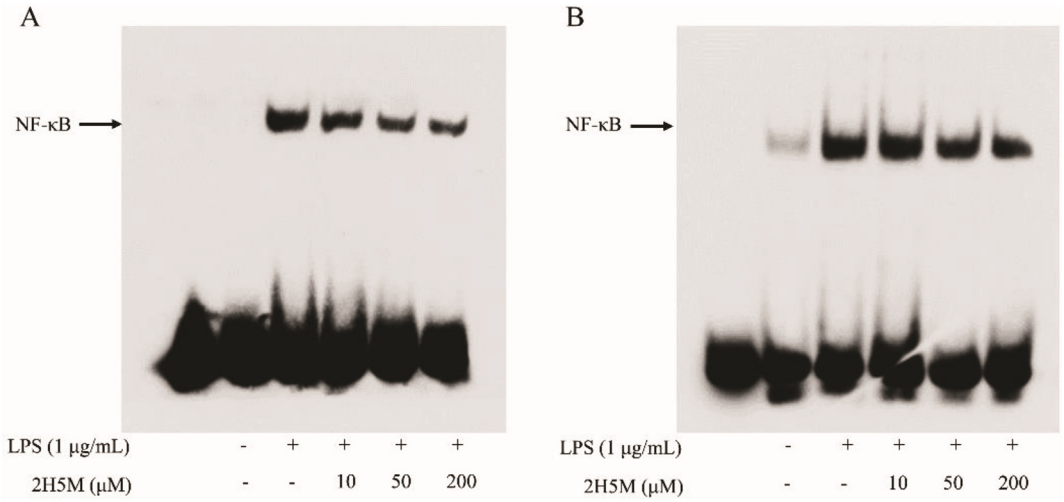

Fig. 6. 2H5M suppressed the NF-κB activity inside the nucleus of NF-κB in LPS-stimulated BV-2 (A) and RAW264.7 (B) cells. Cells were pretreated with 2H5M (10, 50, and 200 μM) for 1 h, and stimulated with LPS (1 μg/mL) for 18 h. EMSA was performed to determine the NF-κB activity in nuclear raction by using DNA probe specific to NF-κB.

observation.

2.10. Molecular docking

The crystal structure of NF-κB (PDB ID: 1IKN) was obtained from PDB database. The protein and ligand molecules were prepared by DS 3.5 respectively before docking. Molecular docking of the 2H5M into the NF-κB protein binding sites was performed by CDOCKER protocol. The negative CDOCKER energy was calculated after conducting the molecular docking (Wu et al., 2003).

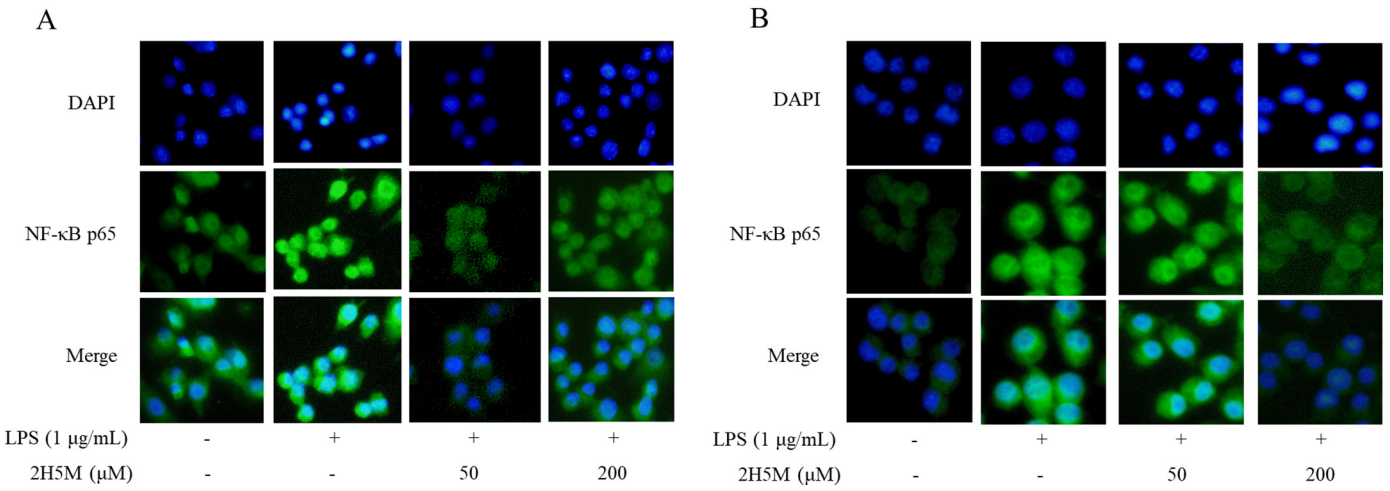

Fig. 7. The effect of 2H5M on translocation of NF-κB p65 in BV-2(A) and RAW 264.7 cells (B). Cells were exposed to 200 μM of 2H5M with LPS. Nucleus was stained with DAPI and NF-κB p65 was immunostained with p65 antibody.

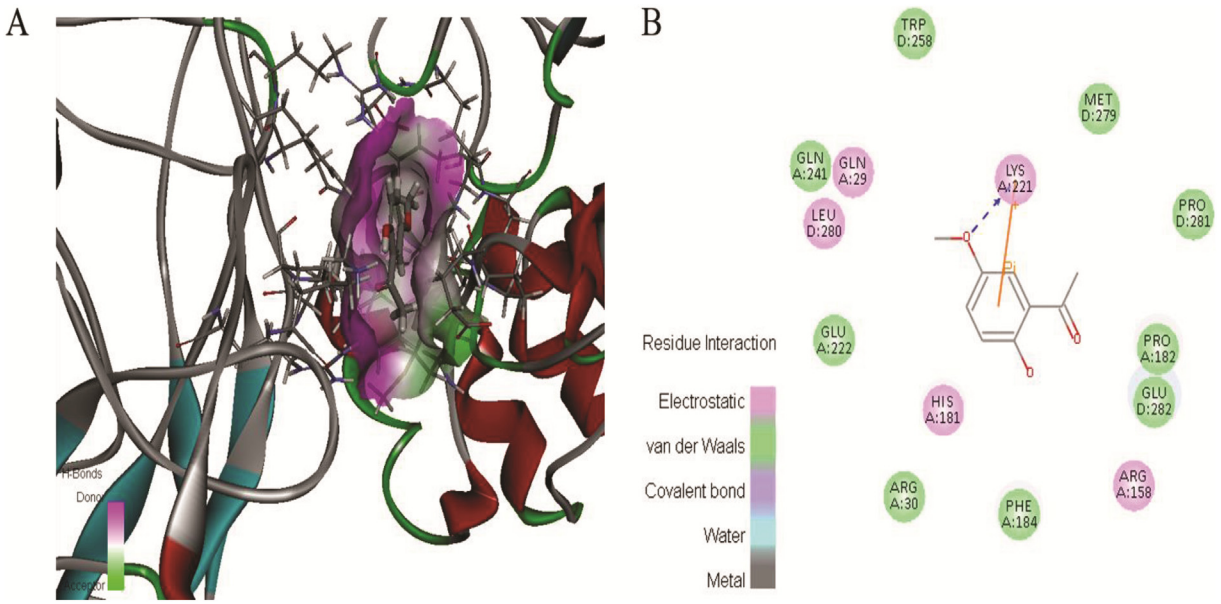

Fig. 8. Binding pose of 2H5M with NF-κB (A). The important residues formed between 2H5M and NF-κB formed with (B). Hydrogen bonds formed with LYS 221 (Blue arrow). (For interpretation of the references to colour in this figure legend, the reader is referred to the web version of this article.)

2.11. Statistics

All results were expressed as the means ± SD ($n = 3$). Differences between groups were calculated by One-way analysis of variance (ANOVA) and *t*-test. A value of $p < .05$ was considered statistically significant.

3. Results

3.1. Elucidation of 2H5M

2H5M: 2'-Hydroxy-5′- Methoxyacetophenone: ^{1}H NMR (DMSO-d_6, 500 MHz): δH12.05 (2-OH, s), 7.71 (H-6, d, 3.0), 7.23 (H-4, dd, 9.0, 3.0), 7.01 (H-3, d, 9.0), 3.85 (5-OCH3, s), 2.42 (1-COCH3, s). ^{13}C NMR (DMSO-d_6, 125 MHz): δ_C 203.8 (1-COCH3), 156.3 (C-2, s), 151.4 (C-5, s), 123.7 (C-4, d), 123.4 (C-1, s), 118.9 (C-3, d), 113.3 (C-6, d), 56.6 (5-OCH_3), 26.4 (1-$COCH_3$). The chemical structure of 2H5M was shown in Fig. 1A. The NMR data of 2'-Hydroxy-5′-Methoxyacetophenone was showed as following and compared with previous report (Patra et al., 1987).

3.2. Cytotoxicity of 2H5M on cells

In order to ascertain whether 2H5M exerted cytotoxicity on BV-2 and RAW264.7 cells, the MTT assay was performed. As shown in Fig. 2B and C, no significances were observed in all tested groups with various dose of 2H5M (10, 20, 50, 100, and 200 μM). Therefore, concentrations of 10, 20, 50, 100, and 200 μM of 2H5M were used for the further investigation.

3.3. Effect of 2H5M on NO production

The BV-2 and RAW264.7 cells were exposed to various concentrations of 2H5M (10, 20, 50, 100, and 200 μM) and induced with LPS (1 μg/mL). The NO concentration in various concentration groups were shown in Fig. 2(A, B). The NO concentration was increased when the cells exposed to LPS, and the treatment with 2H5M (50–200 μM) significantly decreased the LPS-induced NO production in BV-2 and

RAW264.7 cells. Briefly, treatment with 2H5M prior to LPS activation could significantly suppress the secretion of NO.

3.4. Effect of 2H5M on levels of TNF-α

To investigate the inhibitory effect of 2H5M on TNF-α production, the cells were treated with LPS in the absence or presence of 2H5M, and the levels were measured by ELISA. As shown in Fig. 2(C, D), compared with un-stimulated cells, the level of TNF-α was increased in LPS-induced cells. Pre-treatment with 10, 50, and 200 μM 2H5M inhibited the production of TNF-α in a dose-dependent manner.

3.5. Effect of 2H5M on ROS production

To determine whether 2H5M can scavenge the ROS, the DCFH-DA assay was carried out. As expected, LPS treatment induced ROS accumulation compared to untreated cells. 2H5M reduced the LPS-stimulated elevation of ROS production, and the DCF fluorescence intensity was significantly decreased in a dose-dependent manner (Fig. 3). Those results indicated that 2H5M markedly attenuates ROS generation in LPS-stimulated BV-2 and RAW264.7 cells.

3.6. Effect of 2H5M on expression of iNOS and COX-2

Since 2H5M could down-regulate NO production, we used western blot to verify whether it reduce NO concentration via down-regulation of iNOS. As shown in Fig. 4(A) and (C), reduction of iNOS protein was consistent with the result of NO production observed in this study in LPS-stimulated cells. Moreover, the level of COX-2 was also investigated. As depicted in Fig. 4(B) and (D), the protein level of COX-2 was dramatically increased by treatment with LPS compared to untreated cells and down-regulated by 2H5M.

3.7. Effect of 2H5M on NF-κB signaling pathway

NF-κB is a major signaling pathway in inflammatory reaction. To examine whether 2H5M could restrain the LPS-induced NF-κB activation, the patterns of IκBα, NF-κB-p65, p-IκBα, and p-NF-κB p65 were detected respectively by Western blot assay. As shown in Fig. 5, the levels of p-I-κBα and p-NF-κB p65 increased in LPS-treated cells, and they were down-regulated by co-treatment with various concentrations of 2H5M, which indicated that 2H5M could inhibit the phosphorylation of I-κBα and NF-κB-p65. In summary, the above results demonstrated that 2H5M could inhibit the activation of the NF-κB pathway in LPS stimulation of BV-2 and RAW264.7 cells.

3.8. Effect of 2H5M on NF-κB DNA bingding activity

To detect the effect of 2H5M on the activity of NF-κB in the nucleus of LPS-induced BV-2 and RAW264.7 cells, EMSA was performed. As shown in Fig. 6, the nuclear level of NF-κB probe binding activity in LPS group was significantly higher than that in the untreated cells. However, the strength of the signal from the NF-κB-DNA complex decreased along with the increase of the concentration of 2H5M. The result demonstrated that 2H5M could inhibit the activity of NF-κB in the nucleus of LPS-induced BV-2 and RAW264.7 cells.

3.9. Effect of 2H5M on NF-κB p65 translocation

To determine the inhibitory effect of 2H5M on the translocation of NF-κB p65, the immunocytochemistry was utilized to evaluate p65 localization. As shown in Fig. 7, in blank group, the green fluorescence was faint in nucleus and intense in cytoplasm. Induced by LPS, cells were larger in size and the fluorescence was opposite from blank group, indicating that the p65 has translocated from cytoplasm into nucleus. After treatment with 2H5M and stimulated with LPS, the green fluorescence in nucleus was weakened with the increasing dose of 2H5M. Those results suggested that 2H5M could inhibit the translocation of NF-κB p65.

3.10. Docking study of NF-κB with 2H5M

Molecular docking study was demonstrated to investigate the interaction between 2H5M and NF-κB. Fig. 8 showed the docked pose of 2H5M with NF-κB with a CDOCKER energy of −23.466 kcal/mol. And 2H5M formed one hydrogen bond NF-κB at Lys221 with a distance of 5 Å.

4. Discussion

Inflammation is a complex pathologic process of body to eliminate harmful stimuli, however, prolonged inflammation has been seemed as one of the major causes of several diseases (Chen et al., 2018). Neuroinflammation regulated by microglia cells is always considered as a chief culprit of neurodegenerative diseases, therefore, interference in over-activation of microglia cells is a useful way to control the neuroinflammatory reaction (Geng et al., 2017).

NO is synthesized from L-arginine catalyzed by NO synthase (NOS). The neuronal NOS (nNOS) is mostly expressed in neural tissue and endothelial NOS (eNOS) is constitutively produced in many cell types, while iNOS is upregulated during abnormal state (Murphy and Gibson, 2007). NO is a two edged sword in inflammatory diseases depending on its origin and production. For example, low concentration of NO generated by eNOS or nNOS is good for physical health because NO exerts antimicrobial activity, and regulates cell signaling and survival. However, a large amount of NO produced by iNOS are related to inflammatory reaction. Moreover, NO causes negative influence on tissue due to its cytostatic or cytotoxic for neighboring cells as well as the invading microorganisms (Tripathi et al., 2007). Furthermore, NO can interact with other radicals to generate cytotoxic molecules. Hence, inhibition of NO production is an anti-inflammatory treatment (Hofseth, 2008). In our study, 2H5M negatively regulated the production of NO in both cells via inhibiting the iNOS expression.

COX, one of the most predominate targets of NSAIDs, is rapidly induced by various stimuli and then contributes to the formation of prostaglandin (PG) associated with inflammation (Badri et al., 2016). COX-1, constitutively expressed in nearly all tissues, is responsible for basal level of prostaglandin E (PGE), while COX-2 is produced by stimuli and the excessive expression of COX-2 could promote neuronal injury, neurodegeneration and cognitive deficits. Moreover, inhibition of COX-2 activity has neuro-protective effect in rodent models of stroke and Parkinson's disease (PD) (Liang et al., 2007). With the addition of 2H5M, the can down-regulate the expression of COX-2 in LPS-stimulated BV-2 and RAW264.7 cells. Activated BV-2 and RAW264.7 cells can trigger the release of inflammatory cytokines, such as TNF-α. And the excessive production of inflammatory cytokines can cause organic damage (Li et al., 2017). In this study, an in vitro model of inflammation was induced by LPS in BV-2 and RAW264.7 cells, and treatment with different concentrations of 2H5M. The results demonstrated that 2H5M significantly suppress the secretion of TNF-α in LPS-stimulated BV-2 and RAW264.7 cells.

ROS is an important molecular target of inflammatory diseases. ROS produced in LPS-induced cells can cause pro-inflammatory response by up-regulating pro-inflammatory cytokines and functioning as a secondary messenger in following progression (Block et al., 2007). Previous study suggested that ROS produced from activated microglia exert cytotoxicity to neurons though protein and lipid oxidation, and it can interact with NO to produce much more deadly intermediates, which lead to neurotoxic damage and become the pathological characters of neurogenesis diseases (Cobourne-Duval et al., 2016). Therefore, ROS regulation has been deemed as a major method to study inflammation (Ko et al., 2017). In the study, 2H5M did scavenge the ROS

production in both cells.

NF-κB promote the production of inflammatory mediators. NF-κB is normally sequestered in the cytoplasm and associated with IκBs. Once stimulated, NF-κB members become activated and then translated to the nucleus to function as transcriptional factors. A large number of investigations regard deregulated NF-κB as a main reason for inflammation (Zhang and Sun, 2015; Kirchner et al., 2018; Wang et al., 2011). In the study, the expression of p-p65 and p-IκB were investigated and the p65 protein translocation was also studied, which indicated 2H5M can suppress the NF-κB activation. And EMSA experiments demonstrated a direct interference of 2H5M on NF-κB DNA binding activity in LPS-stimulated BV-2 and RAW264.7 cells. Therefore, induction of anti-inflammatory responses by 2H5M may be dependent on the NF-κB signaling pathway.

Additionally, it has been well confirmed that the presence of methoxy (-OCH_3) group often enhances the anti-inflammatory activity of compounds. As shown in Fig. 8, 2H5M located in the NF-κB cavity and surrounded by fourteen amino acid residues. Among these amino acid, Gln241, Glu222, Arg30, Phe184, Glu282, Pro182, Pro281, and Met279 were involved in van der Waals interaction, while Gln29, Leu280, His181, Arg158, and Lys221 were involved in hydrogen bonding and electrostatic interaction. The methoxy group of 2H5M was oriented towards Lys221 and a hydrogen bond was formed between them with the distance of 5 Å. Thus, the essential driving forces of 2H5M binding to NF-κB were mainly electrostatic forces in nature. And the CDOCKER energy between methoxy group of 2H5M and NF-κB was with a high negative values. Combining the results 2H5M into the active site of NF-κB, causing conformational changes in NF-κB, which might be the main mechanism of inhibition. These results which indicated that 2H5M may be a good inhibitor of NF-κB due to the hydrogen bonds formed between 2H5M and NF-κB. Moreover, hydroxyl along with ketone groups are able to scavenge neuro-toxicradical species by donating electrons (Himaya et al., 2012). In conclusion, we studied the anti-inflammatory effect of 2H5M in LPS-stimulated BV-2 and RAW264.7 cells. 2H5M can reduce the concentration of NO by down-regulating the expression of iNOS. It also negatively regulate of COX-2, TNF-α as well as ROS production. Moreover, in terms of signaling pathway, 2H5M inhibited the phosphorylation of p65 and IκB and ERK. Furthermore, EMSA showed a direct interference of 2H5M on NF-κB DNA binding activity and the molecular docking indicated the 2H5M could interact with NF-κB. Those observations indicated that 2H5M may be have a potential to be selected as an anti-inflammatory agent.

Conflicts of interest

The authors declare no conflict of interest.

Acknowledgments

The study was supported by the Yangfan Scarce Top Talent Project of Guangdong Province (201433009) and the Program for Scientific Research Start-Up Funds of Guangdong Ocean University [to Zhong-Ji Qian] and supported by Development Project about Marine Economy Demonstration of Zhanjiang City (2017C8B1).

References

Badri, W., Miladi, K., Nazari, Q.A., Greige-Gerges, H., Fessi, H., Elaissari, A., 2016. Encapsulation of NSAIDs for inflammation management: overview, progress, challenges and prospects. Int. J. Pharm. 515, 757–773.

Block, M.L., Zecca, L., Hong, J.S., 2007. Microglia-mediated neurotoxicity: uncovering the molecular mechanisms. Nat. Rev. Neurosci. 8, 57–69.

Chen, L., Shen, X.R., Chen, G., Cao, X., Yang, J., 2015. Effect of three-spot seahorse petroleum ether extract on lipopolysaccharide induced macrophage RAW264.7 inflammatory cytokine nitric oxide and composition analysis. J Oleo Sci. 64, 933–942.

Chen, W.-W., Zhang, X., Huang, W.J., 2016. Role of neuroinflammation in neurodegenerative diseases (review). Mol. Med. Rep. 13, 3391–3396.

Chen, L., Deng, H., Cui, H., Fang, J., Zuo, Z., Deng, J., Li, Y., Wang, X., Zhao, L., 2018. Inflammatory responses and inflammation-associated diseases in organs. Oncotarget 9, 7204–7208.

Cheung, R.C.F., Ng, T.B., Wong, J.H., Chen, Y., Chan, W.Y., 2016. Marine natural products with anti-inflammatory activity. Appl. Microbiol. Biotechnol. 100, 1645–1666.

Cobourne-Duval, M.K., Taka, E., Mendonca, P., Bauer, D., Soliman, K.F.A., 2016. The antioxidant effects of thymoquinone in activated BV-2 murine microglial cells. Neurochem. Res. 41, 3227–3238.

Geng, Y., Zhu, S., Cheng, P., Lu, Z.M., Xu, H.Y., Shi, J.S., Xu, Z.H., 2017. Bioassay-guided fractionation of ethyl acetate extract from *Armillaria mellea* attenuates inflammatory response in lipopolysaccharide (LPS) stimulated BV-2 microglia. Phytomedicine 26, 55–61.

Ginhoux, F., Lim, S., Hoeffel, G., Low, D., Huber, T., 2013. Origin and differentiation of microglia. Front. Cell. Neurosci. 7 (45), 1–14.

Guo, Z., Lin, D., Guo, J., Zhang, Y., Zheng, B., 2017. In vitro antioxidant activity and in vivo anti-fatigue effect of sea horse (Hippocampus) peptides. Molecules 22, 482.

Himaya, S.W.A., Ryu, B., Qian, Z.J., Li, Y., Kim, S.K., 2011. 1-(5-bromo-2-hydroxy-4-methoxyphenyl)ethanone [SE1] suppresses pro-inflammatory responses by blocking NF-κB and MAPK signaling pathways in activated microglia. Eur. J. Pharmacol. 670, 608–616.

Himaya, S.W.A., Ryu, B., Qian, Z.J., Kim, S.K., 2012. Paeonol from *Hippocampus kuda* Bleeler suppressed the neuro-inflammatory responses in vitro via NF-κB and MAPK signaling pathways. Toxicol. in Vitro 26, 878–887.

Hofseth, L.J., 2008. Nitric oxide as a target of complementary and alternative medicines to prevent and treat inflammation and cancer. Cancer Lett. 268, 10–30.

Kang, N., Kim, S.Y., Rho, S., Ko, J.Y., Jeon, Y.J., 2017. Anti-fatigue activity of a mixture of seahorse (*Hippocampus abdominalis*) hydrolysate and red ginseng. Fish. Aquat. Sci. 20, 3.

Kim, M.G., Yang, J.Y., Lee, H.S., 2013. Acaricidal potentials of active properties isolated from *Cynanchum paniculatum* and *Acaricidal* changes by introducing functional radicals. J. Agric. Food Chem. 61, 7568–7573.

Kirchner, J., Brüne, B., Namgaladze, D., 2018. AICAR inhibits NFκB DNA binding independently of AMPK to attenuate LPS-triggered inflammatory responses in human macrophages. Sci. Rep. 8, 7801.

Ko, E.Y., Cho, S.H., Kwon, S.H., Eom, C.Y., Jeong, M.S., Lee, W., Kim, S.Y., Heo, S.-J., Ahn, G., Lee, K.P., Jeon, Y.-J., Kim, K.-N., 2017. The roles of NF-κB and ROS in regulation of pro-inflammatory mediators of inflammation induction in LPS-stimulated zebrafish embryos. Fish Shellfish Immunol. 68, 525–529.

Li, Y., He, S., Tang, J., Ding, N., Chu, X., Cheng, L., Ding, X., Liang, T., Feng, S., Rahman, S.U., Wang, X., Wu, J., 2017. Andrographolide inhibits inflammatory cytokines secretion in LPS-stimulated RAW264.7 cells through suppression of NF-κB/MAPK signaling pathway. Evid. Based Complement. Alternat. Med. 2017, 1–9.

Li, M.Y., Sun, L., Niu, X.T., Chen, X.M., Tian, J.X., Kong, Y.D., Wang, G.Q., 2018. Astaxanthin protects lipopolysaccharide-induced inflammatory response in Channa argus through inhibiting NF-κB and MAPKs signaling pathways. Fish Shellfish Immunol. 86, 280–286.

Liang, X., Wu, L., Wang, Q., Hand, T., Bilak, M., McCullough, L., Andreasson, K., 2007. Function of COX-2 and prostaglandins in neurological disease. J. Mol. Neurosci. 33, 94–99.

Lo Faro, M.L., Fox, B., Whatmore, J.L., Winyard, P.G., Whiteman, M., 2014. Hydrogen sulfide and nitric oxide interactions in inflammation. Nitric Oxide 41, 38–47.

Mammana, S., Fagone, P., Cavalli, E., Basile, M., Petralia, M., Nicoletti, F., Bramanti, P., Mazzon, E., 2018. The role of macrophages in neuroinflammatory and neurodegenerative pathways of Alzheimer's disease, amyotrophic lateral sclerosis, and multiple sclerosis: pathogenetic cellular effectors and potential therapeutic targets. Int. J. Mol. Sci. 19, 831.

Minogue, A.M., 2017. Role of infiltrating monocytes/macrophages in acute and chronic neuroinflammation: effects on cognition, learning and affective behaviour. Prog. Neuro-Psychopharmacol. Biol. Psychiatry 79, 15–18.

Murphy, S., Gibson, C.L., 2007. Nitric oxide, ischaemia and brain inflammation. Biochem. Soc. Trans. 35 (5), 1133–1137.

Muthuramalingam, K., Kim, S.Y., Kim, Y., Kim, H.S., Jeon, Y.J., Cho, M., 2019. Bigbelly seahorse (Hippocampus abdominalis)-derived peptides enhance skeletal muscle differentiation and endurance performance via activated P38MAPK/AKT signalling pathway: an in vitro and in vivo analysis. J. Funct. Foods 52, 147–155.

Neranjan Tharuka, M.D., Bathige, S.D.N.K., Oh, M., Lee, S., Kim, M.J., Priyathilaka, T.T., Lee, J., 2019. Molecular characterization and expression analysis of big-belly seahorse (*Hippocampus abdominalis*) interleukin-10 and analysis of its potent anti-inflammatory properties in LPS-induced murine macrophage RAW 264.7 cells. Gene 685, 1–11.

Oh, Y., Ahn, C.B., Yoon, N.Y., Nam, K.H., Kim, Y.K., Je, J.Y., 2018. Protective effect of enzymatic hydrolysates from seahorse (Hippocampus abdominalis) against H2O2-mediated human umbilical vein endothelial cell injury. Biomed. Pharmacother. 108, 103–110.

Patra, A., Ghosh, G., Sengupta, P.K., Nath, S., 1987. Carbon-13 NMR spectral studies on chalcones and acetophenones. Magn. Reson. Chem. 25, 734–736.

Qian, Z.J., Ryu, B., Kim, M.M., Kim, S.K., 2008. Free radical and reactive oxygen species scavenging activities of the extracts from seahorse, *Hippocampus kuda* Bleeler. Biotechnol. Bioproc. Eng. 13, 705–715.

Qian, Z.J., Kang, K.H., Kim, S.K., 2012. Isolation and antioxidant activity evaluation of two new phthalate derivatives from seahorse, *Hippocampus Kuda* Bleeler. Biotechnol. Bioproc. Eng. 17, 1031–1040.

Ryu, B., Qian, Z.J., Kim, S.K., 2010. Purification of a peptide from seahorse, that inhibits TPA-induced MMP, iNOS and COX-2 expression through MAPK and NF-κB activation, and induces human osteoblastic and chondrocytic differentiation. Chem. Biol. Interact. 184, 413–422.

Sevenich, L., 2018. Brain-resident microglia and blood-borne macrophages orchestrate central nervous system inflammation in neurodegenerative disorders and brain cancer. Front. Immunol. 9, 697.
Tripathi, P., Tripathi, P., Kashyap, L., Singh.V., 2007. The role of nitric oxide in inflammatory reactions. FEMS Immunol. Med. Microbiol. 51, 443–452.
Tsaryk, R., Peters, K., Barth, S., Unger, R.E., Scharnweber, D., Kirkpatrick, C.J., 2013. The role of oxidative stress in pro-inflammatory activation of human endothelial cells on Ti6Al4V alloy. Biomaterials. 34, 8075–8085.
Wang, Y.P., Wu, Y., Li, L.Y., Zheng, J., Liu, R.G., Zhou, J.P., Yuan, S.Y., Shang, Y., Yao, S.L., 2011. Aspirin-triggered lipoxin A4 attenuates LPS-induced pro-inflammatory responses by inhibiting activation of NF-κB and MAPKs in BV-2 microglial cells. J. Neuroinflammation 8, 95.
Wu, G., Robertson, D.H., Brooks, C.L., Vieth, M., 2003. Detailed analysis of grid-based molecular docking: a case study of CDOCKER A CHARMm-based MD docking algorithm. J. Comput. Chem. 24, 1549–1562.
Ye, J., Ye, C., Huang, Y., Zhang, N., Zhang, X., Meitian, X., 2018. *Ginkgo biloba* sarcotesta polysaccharide inhibits inflammatory responses through suppressing both NF-κB and MAPK signaling pathway. J. Sci. Food Agric. https://doi.org/10.1002/jsfa.9431.
Zhang, H., Sun, S.-C., 2015. NF-κB in inflammation and renal diseases. Cell Biosci. 5, 63.
Zhang, Y.Y., Ryu, B.M., Qian, Z.J., 2017. A review - biology, aquaculture and medical use of seahorse, Hippocampus spp. Annu. Rev. Cell Dev. Biol. 14, 1–12.